Journal listed in Halu Oleo University Journal System

International Journal of Acta Material

Int. J. Act. Mat.

homepage: https://ijacmat.uho.ac.id/index.php/journal

Research Article

Effect of pH and Stirring Speed on the γ-Fe_2O_3 Material Properties Synthesized from Iron Sand by Using Co-Precipitation Method

, L. Agusu[a]*, Amiruddin[b], M. Nalis[a]

[a] *Department of Physics, Faculty of Mathematics and Natural Sciences, Halu Oleo University, Kampus Hijau Bumi Tridharma, Anduonohu, Kendari, Sulawesi Tenggara 93232, Indonesia*

[b] *Department of Chemistry, Faculty of Mathematics and Natural Sciences, Halu Oleo University, Kampus Hijau Bumi Tridharma, Anduonohu, Kendari, Sulawesi Tenggara 93232, Indonesia*

Corresponding Author: la_agusu@yahoo.com

Article info

Received: June 2024
Received in revised: June 2024
Accepted: August 2024
Available online: August 2024

Abstract

Research has been conducted to investigate the impact of pH and stirring on the magnetic properties of γ-Fe_2O_3 nanoparticles derived from iron sand using the co-precipitation method. The objective of this study was to synthesize γ-Fe_2O_3 nanoparticles and examine how pH and stirring affect their size and properties. The co-precipitation method involved mixing iron sand with HCl as a solvent and NH_4OH as a precipitator. The experimental setup included variations in pH, specifically pH 10 and pH 12, as well as stirring speeds of 600 rpm and 700 rpm. The synthesized maghemite nanoparticles were characterized using XRD (X-Ray Diffraction), SEM (Scanning Electron Microscope), and VSM (Vibrating Sample Magnetometer) techniques. XRD analysis revealed that the particle size at 600 rpm under pH 10 was 52.085 nm, whereas at 700 rpm under pH 12 it was 47.821 nm. The VSM characterization results demonstrated a remanent magnetization of 25.5 emu/gr, a coercivity field of -0.01 Tesla, and a saturation magnetization of 52.45 emu/gr. This study confirmed that the maghemite nanoparticles produced exhibited ferromagnetic properties.

Keywords: Iron sand, co-precipitation method, pH, γ-Fe_2O_3, ferromagnetic

INTRODUCTION

The development and progress in the field of science and technology are closely tied to the increasing needs of humans. As a result, the advancement of technology today requires new materials with unique properties. Currently, there is significant research being conducted in the field of nanomaterial due to their wide applications in microelectronics, sensors, optical systems, medical devices, semiconductors, and more. In Indonesia, research in the field of nano materials or nano technology is still in its early stages due to limited funding and experimental facilities. These challenges necessitate diligent efforts to harness the country's resource potential (Chauhan et al., 2024; Ji et al., 2024; Revathy, Sajini, Augustine, & Joseph, 2023).

On the other hand, Indonesia possesses abundant natural resources, including iron sand, which is currently only utilized as a building material. However, it has been discovered that iron sand contains Fe_3O_4 or ferrite, a soft magnetic material. This compound exhibits controllable magnetic properties through the addition of other cations with varying degrees of magnetism. Nano-sized iron sand (Fe_3O_4) possesses ferrimagnetic properties that offer a wide range of potential applications. The use of iron sand (Fe_3O_4) with nano particle size presents an alternative solution to meet the growing demands for raw materials in the developing electronics industry (Li, Huang, Cui, Jin, & Xu, 2024).

Magnetic nano particles Fe_3O_4 have been extensively developed for various applications, such as ferrogel, radar wave absorbers, shielding, electromagnetic interference, and medical devices in acupressure. In their

application, magnetic nano particles often interact with heat, either directly or from the surrounding environment. The effects of heat on these particles can impact their magnetic properties, and high temperatures can cause changes in their magnetic behavior. These changes are attributed to alterations in crystal structure or phase (Chellappa & Vijayalakshmi, 2019; Jiao et al., 2021).

In recent years, researchers have successfully synthesized Fe_3O_4 nano particles using various methods. For instance, the sol gel method developed by Xu et al., (2007) and the controlled hydrolysis method employed by Iida, Takayanagi, Nakanishi, & Osaka, (2007) for synthesizing Fe_3O_4 nanoparticles. Additionally, Hong, Li, Wang, & Li, (2007) opted for the co-precipitation method in water. Among these synthesis methods, the co-precipitation method is the simplest, involving an easier procedure and a low reaction temperature (<100^{o}C). It is a chemical process used to separate analytes from impurities and has proven to be effective. However, producing Fe_3O_4 particles sometimes presents challenges regarding their size, homogeneity (particle distribution), and morphology (Niu et al., 2024; H. Wang, Jiang, Qin, Xiong, & Zhao, 2024; L. Wang et al., 2021). This study aims to address these issues by investigating the effect of pH and variations in stirring time during the synthesis process. The co-precipitation process is employed in this study due to its time efficiency and the availability of supporting tools.

MATERIALS AND METHODS

Materials and Instrumentation

In this study, the materials utilized included North Konawe natural iron sand, 37% HCl, Methanol, NH_4OH, Aluminum foil, Whatman filter paper, bi-distilled water, and distilled water. The tools employed in this study were various sizes of volume pipettes (pyrex), beakers (pyrex), measuring flasks (pyrex), measuring pipettes (pyrex), and Erlenmeyer flasks (pyrex). Additionally, ovens (Gallenkamp Civilab Australia), analytical scales (Explorer Ohaus: max, 210 g, min 0.1 mg), fillers, Petri dishes, stands, clamps, 50 ml burettes, permanent magnets, magnetic stirrers, stirrers, hot plates, thermometers, pH meters, SEM, XRD, and VSM were employed.

Sample preparation (iron sand)

The iron sand was collected from Tapunggaya Village, Molawe District, North Konawe Regency, Southeast Sulawesi, Indonesia. Subsequently, it underwent a thorough cleaning and separation process utilizing a permanent magnet.

Extraction of γ-Fe_2O_3 by co-precipitation method

The extraction of γ-Fe_2O_3 was conducted using the co-precipitation method with natural iron sand as the starting material. The synthesis process of Fe_2O_3 began with the preparation of sand through the separation of fine sand based on specified weight criteria. The sand, weighed using an analytical balance, amounted to approximately 20 grams. Subsequently, 20 grams of iron sand were placed in a beaker and mixed with 50 ml of HCl (12.063 M). The mixture of iron sand and HCl was stirred using a magnetic stirrer for 120 minutes at a constant temperature of 70 ºC.

Upon completion of the stirring process, the resulting solution was separated from impurities using filter paper. The precipitate obtained from the filtration process was then mixed with NH_4OH (6.5 M) until reaching pH levels of 8.0, 9.0, 10, 11, and 12, respectively. The mixture was stirred for 20 minutes using a magnetic stirrer at a constant temperature of 70-75 ºC.

The solution obtained from the stirring process underwent another round of filtration using filter paper, and the filtration results were repeatedly washed with distilled water to obtain pure Fe_3O_4 powder. Subsequently, the material was dried in an oven at a temperature of 105 ºC for a duration of 24 hours. The Magnetite Fe_3O_4 obtained was divided into two types of samples: powder and pellets. Each sample was then subjected to calcination at various temperatures, specifically 400 ºC for 3 hours, to form Fe_2O_3.

Characterization of γ-Fe_2O_3 derived from iron sand

SEM characterization

Scanning Electron Microscopy (SEM) is a surface analysis technique that employs an electron microscope. The electron beam is generated from the electron transmitter situated at the top of the microscope. SEM operates by focusing the electron waves emitted by the electron gun through the condenser lens, resulting in a clear point of focus achieved by the

objective lens. The energized scanning coil produces a magnetic field for the electron beam. When the electron beam interacts with the sample, it generates secondary electrons which are then collected by either a secondary detector or a backscatter detector. The resulting image displayed on the Cathode Ray Tube (CRT) represents the surface topography, comprising thousands of points with varying intensities.

X-Ray Diffraction (XRD) analysis

The purpose of conducting characterization is to obtain an X-ray diffraction (XRD) pattern. The results of XRD measurements are utilized to determine the phase distribution and phase content of the sample being analyzed. The phase identification process is carried out by comparing data or utilizing the search match method. When a beam of X-rays is directed at a crystal sample, the crystal plane will diffract X-rays that possess the same wavelength as the distance between the crystal lattices. These diffracted rays are captured by a detector and translated into diffraction peaks. The intensity of the diffraction is directly proportional to the number of crystal planes present in the sample. Each peak observed in the XRD pattern represents a crystal plane with a specific orientation in the three-dimensional axis. The resulting peaks from this measurement data are then compared with X-ray diffraction standards for nearly all types of materials.

Analysis using Vibrating Sample Magnetometer (VSM)

The VSM test is conducted to obtain the magnetization curve of a material, either as a function of temperature or external field. This allows for the determination of the material's magnetic phase, magnetic transition temperature, and anisotropic constant. The Vibrating Sample Magnetometer has emerged as a widely utilized instrument for determining the magnetic properties of various nano-sized materials. These properties can be classified into diamagnetic, paramagnetic, ferromagnetic, and antiferromagnetic based on their magnetic characteristics. Diamagnetic materials exhibit negative and very small magnetic susceptibility (k), while paramagnetic materials have positive magnetic susceptibility (k) values greater than 1, which also depend on temperature. Ferromagnetic and antiferromagnetic materials, on the other hand, have positive k values greater than those of paramagnetic materials.

The nanomagnetic behavior is greatly influenced by the particle size, with smaller particles demonstrating enhanced magnetic power. Furthermore, nanomagnetic particles below 10 nm in size exhibit superparamagnetic properties at room temperature. These findings are made possible through processes and tools designed to observe and analyze nanomagnetic properties. One such tool employed to uncover the characteristics of nanomagnetic materials is the Vibrating Scanning Magnetometer (VSM).

RESULTS AND DISCUSSION

Synthesis of γ-Fe_2O_3 nanoparticles from iron sand

The synthesis of γ-Fe_2O_3 nanoparticles was carried out using natural iron sand. The co-precipitation method was employed for this study, which involves precipitating multiple substances together when reaching their saturation point. This method offers simplicity in the synthesis procedure and operates at a lower reaction temperature of 70-75°C.

The synthesis process begins with the separation of iron sand using a permanent magnet, followed by immersion in a 95% ethanol solution to dissolve organic impurities. Subsequently, 20 grams of the separated iron sand was dissolved in 50 mL of HCl (12.063 M) at a constant temperature of 70°C for 120 minutes. HCl, a strong acid, was used as it can dissolve iron oxide from iron ore into Fe^{3+} and Fe^{2+}, resulting in $FeCl_3$ and $FeCl_2$, respectively. This dissolution process is indicated by the formation of a yellow-brown color, which serves as the basis for the synthesis of γ-Fe_2O_3 (Zhou et al., 2023), as shown in the following reaction Equation 1.

$$3Fe_3O_{4(s)} + 8HCl_{(l)} \longrightarrow 2FeCl_{3(l)} + FeCl_{2(l)} + 3Fe_2O_{3(s)} + 3H_2O(l) + H_{2(g)} \quad (1)$$

The reaction solution contains both Fe^{2+} and Fe^{3+} ions, which serve as the foundation for the synthesis of γ-Fe_2O_3. The co-precipitation method is utilized to form nanoparticles from this solution by precipitating it with an NH_4OH base solution (Koizumi, Uddin, & Kato, 2021; Zhou et al., 2023). Carbonate compounds can be employed as precipitants, although NaOH is commonly used. However, a drawback of using NaOH is that Na cations can be absorbed by hydroxide precipitates, making it challenging to

effectively remove these cations during the washing process. The presence of such impurities will adversely affect the quality of the ferrite produced. To eliminate NH_4OH impurities in the precipitate, the precipitate is heated at a high temperature (Ahire et al., 2022). Subsequently, it is stirred using a Magnetic Stirrer for 20 minutes at a constant temperature of 70-75 ºC, resulting in the formation of compounds as indicated by the following reactions Equation 2.

$$2FeCl_{3(l)}+FeCl_{2(l)}+H_2O_{(l)} + 8NH_4OH_{(l)} \longrightarrow Fe_3O_{4(s)} + 8NH_4Cl_{(l)} + 5H_2O_{(l)} \quad (2)$$

Black precipitates form immediately when the first reaction solution is mixed with a base solution, leading to the creation of nano-sized Fe_3O_4 particles. The solution is then filtered using Whatman filter paper and the resulting filtration is washed repeatedly with distilled water to remove Fe_3O_4 powder. Subsequently, it is dried in an oven at a temperature of 105 ºC for 24 hours. To produce γ-Fe_2O_3 particles, a calcination process is conducted at a temperature of 400^{o}C for 4 hours, resulting in the formation of a brick-red powder, which is the characteristic color of γ-Fe_2O_3. The co-precipitation product, in the form of a brick-red powder, exhibits magnetic properties, solubility in acid, and insolubility in water, consistent with the properties of γ-Fe_2O_3. Therefore, based on these findings, it can be concluded that the resulting powder is γ-Fe_2O_3.

The chemical properties of γ-Fe_2O_3, which align with its physical properties, are evident in the reaction that occurs when Fe_2O_3 from natural iron sand is dissolved in HCl (12.063 M). Dissolving γ-Fe_2O_3 from iron sand in HCl (12.063 M) causes decomposition of the Fe ions in the iron sand into Fe^{2+} and Fe^{3+}. The ratio between ferrous ions (Fe^{2+}) and ferric ions (Fe^{3+}) in a basic medium (alkali) significantly influences the synthesis outcomes, including the range of particle size diameters and resulting magnetic properties. The formation of γ-Fe_2O_3 relies on the binding of Fe^{2+} or Fe^{3+} ions with $(OH)^-$ ions derived from the NH_4OH compound (precipitant compound), yielding $Fe(OH)_2$, which then combines with oxygen to produce γ-Fe_2O_3. The reaction equation is as in Equation 3.

$$2FeCl_{3(l)}+FeCl_{2(l)}+H_2O_{(l)}+8NH_4OH_{(l)}+C_2H_4O_{(l)} \longrightarrow Fe_3O_{4(s)} + 8NH_4Cl_{(l)} + 5H_2O_{(l)} \quad (3)$$

The addition of NH4OH is done to precipitate the γ-Fe_2O_3 compound from the solution and to make the solution in a basic condition based on the specified pH. The pH value affects the particle size, where if during the synthesis the pH produced is higher, the particle size produced is expected to be smaller. However, the length of time to synthesize must be considered carefully because if the sample condition is very acidic when added with HCl for too long, it will cause oxidation and the resulting material is no longer γ-Fe_2O_3 (Iida et al., 2007). The relationship between pH and the addition of 8 M NH_4OH solution can be seen in Table 1.

Table 1. Correlation between pH and the addition of 8 M NH_4OH during the γ-Fe_2O_3 extraction process.

pH	Volume HCl (12.073 M)	Volume NH_4OH (8 M)
8	50 mL	85 mL
9	50 mL	145 mL
10	50 mL	210 mL
11	50 mL	340 mL
12	50 mL	575 mL

Table 1 illustrates a positive correlation between the desired pH level and the corresponding volume of NH_4OH added. Subsequently, the stirring process was sustained by maintaining a constant temperature of 70-75ºC until the formation of a γ-Fe_2O_3 precipitate, which could be magnetically attracted (Figure 1). The precipitate was then collected and washed with distilled water to eliminate any residual smell of NH_4OH. Subsequently, the mixture was heated at a temperature of 105ºC for a duration of 24 hours, resulting in the production of γ-Fe_2O_3 powder. Furthermore, the calcination process was carried out in a furnace at a temperature of 400ºC for 3 hours. This step was undertaken to remove any remaining organic solvents present in the Fe_3O_4 precipitate and to oxidize γ-Fe_2O_3, thereby ensuring that the obtained calcination product solely consisted of the desired metal oxide γ-Fe_2O_3.

The γ-Fe_2O_3 particles produced through synthesis using the co-precipitation method are depicted in Figure 1 and exhibit a robust response when approached by a magnetic rod. According to Al-Hakkani, Gouda, & Hassan, (2021), γ-Fe_2O_3 particles are categorized as ferrimagnetic materials with potent magnetic properties. Consequently, they display a significant response when brought into proximity

with a magnetic rod. This response originates from the presence of unpaired electron pairs within the magnetic material's orbital, which is a characteristic of ferrimagnetic materials. The greater the number of unpaired electrons in the d-orbital, the more pronounced the magnetic response to the magnetic field (Basumatary et al., 2024).

During the synthesis of γ-Fe_2O_3, certain variables are maintained constant, including the concentrations of HCl (12.07 M) and NH_4OH (6.5 M), a HCl volume of 50 ml, a maximum temperature of 75ºC, and a stirring time of 120 minutes. Additionally, the NH_4OH solution must be added via titration to prevent the solution from thickening.

Figure 1. γ-Fe_2O_3 particles are attached to a permanent magnet

Characterization of γ-Fe_2O_3 Nanoparticles under Varying pH Conditions

X-Ray Diffraction analysis

X-Ray Diffraction (XRD) is a method commonly used for the characterization of solid materials. It involves the scattering of ionization events at a wavelength of 0.1-200 nm. In this study, XRD analysis was employed to determine the crystalline structure of a material. Initial testing using XRD was conducted to verify the formation of γ-Fe_2O_3 crystals. XRD analysis is typically the first step in characterizing the phase present in powder samples synthesized through the co-precipitation method. This technique allows for the determination of crystal structure and size (Iida et al., 2007; Zhou et al., 2023) .

X-ray diffraction provides valuable information about the structure of polymers, including their amorphous and crystalline states. Polymers can exhibit a combination of crystalline and amorphous regions. Crystalline polymers produce sharp peaks in X-ray diffractograms, while amorphous polymers produce broader peaks. The composition of the compounds comprising the nano γ-Fe_2O_3 particles was identified using the X-ray diffraction method by comparing the 2θ value of the sample with that of the standard. Another method of identification is comparing the d-spacing value of the γ-Fe_2O_3 diffractogram peaks with the d-spacing value of the standard graph. If the 2θ value and the d-spacing value of the sample peaks closely match those of the standard diffraction planes, it can be concluded that the peaks are produced from the same diffraction plane on similar particles.

The product of magnetite oxidation is a reddish-brown powder that is soluble in hydrochloric acid but insoluble in water and ethanol (Munoz, de Pedro, Casas, & Rodriguez, 2015). As observed in Figure 2, the XRD spectrum of the synthesized maghemite exhibits the highest relative intensity peaks at 2θ values of 30.2406° (220), 35.6302° (311), 37.2492° (222), 43.2835° (400), 53.7325° (422), 57.2714° (511), and 62.9250° (440). Based on the characterization results, there is a significant match between the synthesis data and the JCPDS Card No. 39-1346 reference for maghemite. Therefore, it can be concluded that the synthesized substance is maghemite, as depicted in the XRD spectrum shown in Figure 2.

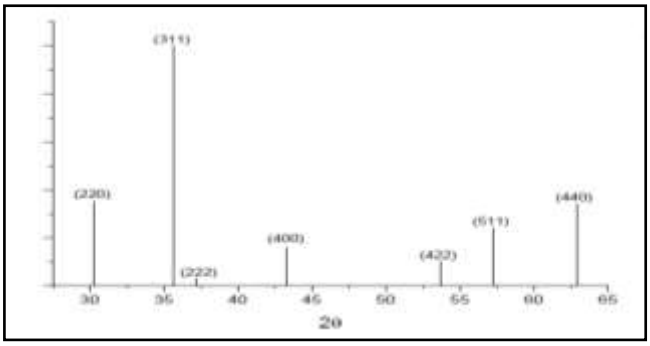

Figure 2. XRD spectrum of maghemite (*JCPDS Card* No. 39-1346)

Based on the data presented in Figure 3, it is evident that the γ-Fe_2O_3 particles formed exhibit a crystalline structure. Notably, the two γ-Fe_2O_3 samples synthesized with different pH levels display similar peak patterns, suggesting that they share the same phase. By employing the Scherrer method and calculating the crystal size of maghemite pH 10 and pH 12 at a stirring speed of 700 rpm, we determined their crystal sizes as 33,483 nm and 47,821 nm, respectively.

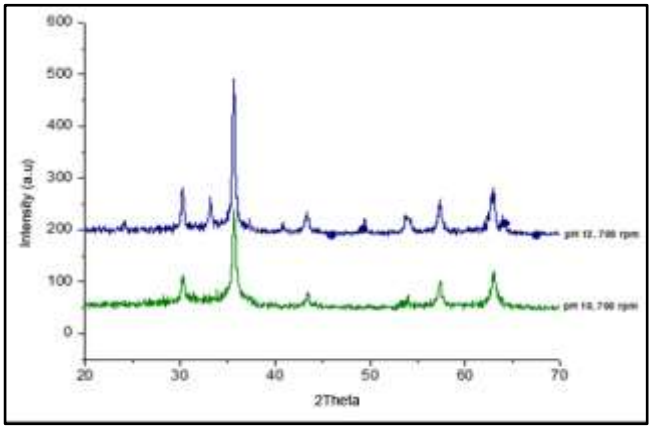

Figure 3. XRD of γ-Fe_2O_3 synthesized at pH variations a). pH 10 stirringfor 700 rpm, b). pH 12 stirring 700 rpm.

Prasetya, (2018) have established that an increase in precipitation pH results in a decrease in crystal size, suggesting an inverse relationship between precipitation pH and crystal size. However, contrary to expectations, the crystal size actually increased when the pH of the precipitation solution was raised in this study. This unexpected outcome raises suspicions regarding the accuracy of the pH meter and the control over the gradual addition of 8 M NH_4OH to the iron oxide solution.

Furthermore, it is important to note that the synthesis of γ-Fe_2O_3 nanoparticles through the co-precipitation method is significantly affected by the ratio of ferrous ions (Fe^{2+}) to ferric ions (Fe^{3+}) in an alkaline medium. These effects encompass the range of particle size diameters as well as the resulting magnetic properties.

SEM analysis

SEM analysis was performed to examine the surface morphology of solid samples. SEM, which utilizes electrons as an imaging source and an electromagnetic field as a lens, is a highly effective analytical technique. Figure 4 displays the SEM image of iron sand samples with varying pH levels, magnified at 20,000x. This analysis aimed to determine the overall morphological characteristics of the sample. In Figure 4, the morphology of γ-Fe_2O_3, synthesized using HCl solvent with 700 rpm stirring at pH 10 and pH 12, is depicted.

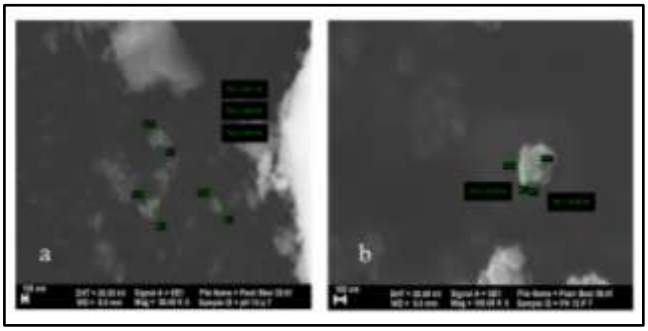

Figure 4. SEM characterization results of γ-Fe_2O_3 synthesized at pH variations (a). pH 10 stirring 700 rpm (b). pH 12 stirring 700 rpm

Based on the observations depicted in the SEM image above, it is evident that there are still aggregates of γ-Fe_2O_3 particles present. This can be attributed to the strong magnetic properties of γ-Fe_2O_3 particles, which cause them to be attracted to and clump together, forming collections of γ-Fe_2O_3 particles (Xu et al., 2007; Zhou et al., 2023).

VSM Analysis

The magnetic properties of magnetic (γ-Fe_2O_3) can be assessed by employing a Vibrating Sample Magnetometer (VSM), an instrument invented by scientist Simon Foner in 1956. The VSM operates based on Faraday's Law of Induction, which stipulates that a changing magnetic field generates an electric field. When a sample is placed on a vertically vibrating rigid rod within a magnetic field H, it becomes magnetized, either permanently or temporarily when subjected to an external magnetic field (H). The vibration of the sample induces alterations in the magnetic force lines, consequently generating an AC voltage signal on the pick-up coil (Pavithra, Nirmala, Priyadharshini, Kavitha, & Kavitha, 2024).

Moreover, this AC signal is detected and processed by the pre-amp circuit and Lock-in amplifier. The Lock-in amplifier's frequency is set to match the vibration frequency of the reference signal emitted by the sample vibration controller. This Lock-in amplifier reads the voltage signal from the coil that is in phase with the reference signal. All these components are connected to computer software, allowing for the determination of a material's magnetic properties. The results of the VSM test, depicted in Figure 5, are presented in the form of a hysteresis curve.

Important quantities for determining magnetic properties based on hysteresis curves include saturation magnetism (Ms), coercive field (Mc), and remanent magnetization (Mr). The remanent magnetization, also known as saturated magnetization, indicates the ability of nanoparticles to maintain the direction of their magnetic domains when subjected to an external magnetic field. The coercive field represents the magnitude of the field required to reduce magnetization to zero. A higher coercive field value indicates stronger magnetic properties. Remanence, on the other hand, reflects the magnitude of the remaining magnetic field when the external magnetic field is removed.

The results obtained from the vibrating sample magnetometer (VSM) shown in Figure 5 demonstrate that γ-Fe_2O_3 particles at pH 10 with stirring at 700 rpm and pH 12 with stirring at 700 rpm can be classified as soft magnets. This is evident from the almost symmetrical reverse order of the hysteresis curve when subjected to a magnetic field or when the magnetic field is removed, as well as the narrow area of the hysteresis curve. The area of the hysteresis curve indicates the energy required for magnetization. In the case of soft magnets, magnetization requires very little energy. Furthermore, the nanoparticles of γ-Fe_2O_3 remain ferrimagnetic, although their properties can potentially change to superparamagnetic depending on their size.

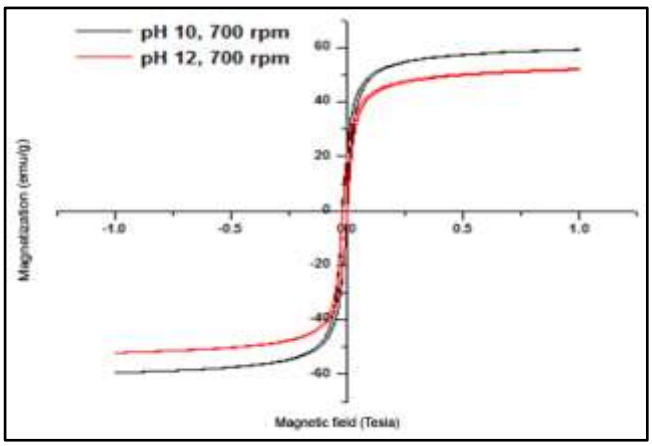

Figure 5. Hysteresis curve of γ-Fe_2O_3 resulting from pH variations a). pH 10 stirring 700 rpm, b). pH 12 stirring 700 rpm.

To be classified as superparamagnetic, a material must not only have a size below 10 nm but also possess a coercive field (Hc) value of 0 (Perdana, 2010). In the case of γ-Fe_2O_3 particles, their Hc value of -0.1 Tesla confirms their ferrimagnetic nature. The remanent magnetization value and saturation magnetization of γ-Fe_2O_3 particles are respectively 24.5 emu/gram and 52.25 emu/g, indicating a favorable level of magnetization.

Characterization of γ-Fe_2O_3 nanoparticles under varying stirring speeds

X-ray Diffraction (XRD) Analysis

Generally, iron sand primarily consists of iron oxide, silicon oxide, and other minor compounds. The composition of the sand content can be determined through testing, such as utilizing XRD. The oxidation of magnetite yields a reddish-brown powder that is soluble in hydrochloric acid but insoluble in water and ethanol (Xu et al., 2007). As depicted in Figure 6, the XRD spectrum of the synthesized maghemite displays high peaks at 2θ values of 30.2406° (220), 35.6302° (311), 37.2492° (222), 43.2835° (400), 53.7325° (422), 57.2714° (511), and 62.9250° (440). Based on the characterization findings, there is a concurrence between the synthesis data and the JCPDS (Joint Committee Powder Diffraction Standard) Card No. 39-1346 reference for maghemite. Therefore, it can be concluded that the synthesized substance is maghemite, as illustrated in Figure 6.

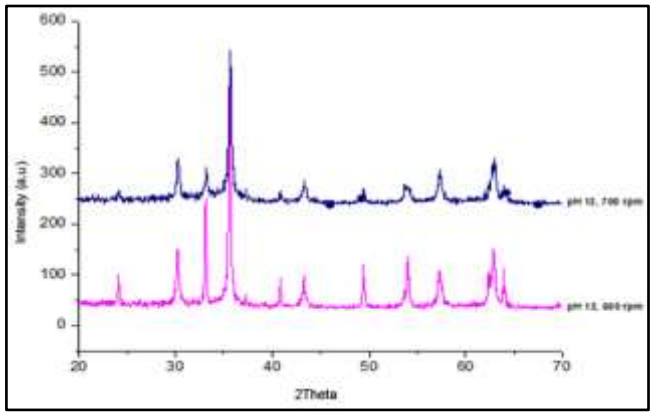

Figure 6. XRD γ-Fe_2O_3 synthesis results from stirring variations a). Stirring 600 rpm pH 12, b). Stirring 700 rpm pH 12

Based on Figure 6, it is evident that there is a marginal difference in the distribution of crystal sizes for stirring speeds of 600 rpm and 700 rpm at pH 12. The average decrease in crystal size is slightly more pronounced for the phenomenon at a stirring speed of 700 rpm and pH 12. Furthermore, the γ-Fe_2O_3 particles formed exhibit a crystalline structure. Both samples of γ-Fe_2O_3

synthesized with variations in pH display similar peak patterns, indicating that they share the same phase. The crystal sizes of maghemite were calculated using the Scherrer method and were found to be 52.058 nm and 47.821 nm for stirring speeds of 600 rpm and 700 rpm at pH 12, respectively.

The stirring speed has an impact on the crystal size of iron oxide particles due to the occurrence of centrifugal force during stirring, which facilitates homogeneous distribution of atoms. Titanium atoms, being reactive to oxygen, bind with oxygen to form oxide molecules during stirring, initiating nucleation. The homogeneity of the solution ensures even nucleation throughout, resulting in nearly uniform particle sizes (Prasetya, 2018). At a stirring speed of 600 rpm, there is an adequate content of $(OH)^-$ (basic atmosphere), causing Fe^{2+} ions to bind with OH- and precipitate as FeO(OH) compound before binding with $Fe(OH)_2$ to form γ-Fe_2O_3. At this stirring speed, there is still one noise suspected to be an impurity compound. On the other hand, at a stirring speed of 700 rpm, it appears that pH 12 is the most suitable condition for the formation of γ-Fe_2O_3, as it optimizes the presence of Fe^{2+}, Fe^{3+}, and $(OH)^-$ ions, resulting in the formation of pure γ-Fe_2O_3 powder without any impurity precipitation.

SEM analysis

Based on observations, it is evident that the wetting process, as the initial coating process, significantly influences the distribution of the nanoparticle coating size. During this process, there is a tendency for the separation of Fe oxide powder into nano-sized particles, which tend to aggregate due to strong particle interactions (Affandi, Mujamilah, Kurniati, & Sudaryanto, 2019). This aggregate formation is illustrated in Figure 7.

The SEM results depicted in Figure 6 demonstrate the presence of aggregates at a stirring speed of 600 rpm, while aggregate formation decreases at a stirring speed of 700 rpm. This phenomenon can be attributed to the influence of stirring speed on particle distribution. During the stirring process, centrifugal force is generated, leading to a homogeneous distribution of atoms. Iron atoms, known for their reactivity to oxygen, form oxide molecules by binding with oxygen when subjected to stirring. This oxide molecule formation initiates nucleation.

The uniformity of the solution promotes nucleation at all points, resulting in the creation of particles with nearly identical sizes (Prasetya, 2018). This finding aligns with the statement made by Affandi et al., (2019), suggesting that an increase in initial stirring speed has a relatively minor impact on the final particle size distribution.

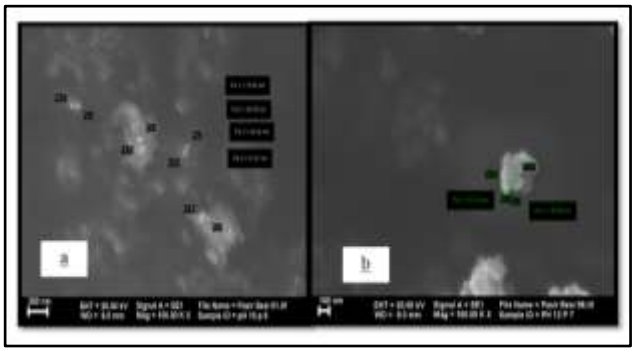

Figure 7. SEM of γ-Fe_2O_3 synthesis results from variations in stirring speed a). Stirring 600 rpm pH 12 b). Stirring 700 rpm pH 12

However, a more detailed examination reveals that higher stirring speeds tend to yield more homogeneous particle sizes, ultimately leading to a stable nano particle size value.

VSM analysis

Important quantities in determining magnetic properties based on hysteresis curves are saturation magnetism (Ms), coercive field (Mc), and remanent magnetization (Mr). The remanent magnetization value, commonly known as saturation magnetization, indicates the ability of nanoparticles to maintain the direction of their magnetic domains when subjected to an external magnetic field. The coercive field is the magnitude of the field needed to reduce its magnetization to zero. A higher coercive field value corresponds to stronger magnetic properties. Remanence indicates the magnitude of the remaining magnetic field when the external magnetic field is removed.

Based on Figure 8, obtained through VSM analysis, it is evident that the 600 rpm pH 10 stirrer and the 700 rpm pH 12 stirrer exhibit similar levels of magnetization. This is evident from the nearly symmetrical reverse sequence of the hysteresis curve when subjected to a magnetic field or when the magnetic field is removed. The narrow area of the hysteresis curve also indicates the energy required for magnetization.

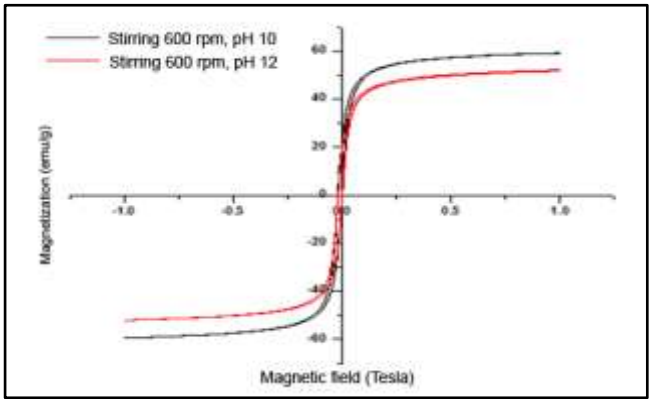

Figure 8. Hysteresis curve of γ-Fe_2O_3 synthesis results from stirring variation and pH influence a). Stirring speed 600 rpm pH 12, b). Stirring speed 700 rpm pH 12

In the case of soft magnets, magnetization requires very little energy. The nano particles of γ-Fe_2O_3 remain ferrimagnetic, although their properties can be changed to superparamagnetic based on their size. A material can be classified as superparamagnetic if it has a coercive field value (Hc) of 0 (Perdana, 2010). The Hc value of γ-Fe_2O_3 particles is -0.1 Tesla, which indicates that they are ferrimagnetic. The remanent magnetization value of γ-Fe_2O_3 particles and the saturation magnetization are 25.5 emu/gram and 52.45 emu/gram, respectively, indicating a high level of magnetization.

CONCLUSION

Maghemite (γ-Fe_2O_3) crystals have been successfully synthesized using the co-precipitation method. These crystals exhibit a brick red color and possess magnetic properties. The highest intensity of the crystals occurs at a diffraction angle of 2θ=35.630, which is a characteristic feature of the γ-Fe_2O_3 particle pattern. The size of the γ-Fe_2O_3 crystals tends to increase as the pH level increases. At pH 10 and pH 12 with 700 rpm stirring, the crystal sizes measure 33.483 nm and 47.821 nm, respectively. Furthermore, the crystal size tends to be smaller when the stirring speed is increased. For instance, at stirring speeds of 600 rpm and 700 rpm with pH 12, the crystal sizes measure 52.058 nm and 47.821 nm, respectively.

REFERENCES

Affandi, S., Mujamilah, M., Kurniati, M., & Sudaryanto, S. (2019). Efek kondisi pembasahan dalam pembentukan nanosfer berbasis oksida besi dan pla. *Jurnal Sains Materi Indonesia*, *Special edition*(0), 156–161. https://doi.org/ 10.17146/jusami.2007.0.0.5131

Ahire, S. A., Bachhav, A. A., Pawar, T. B., Jagdale, B. S., Patil, A. V., & Koli, P. B. (2022). The Augmentation of nanotechnology era: A concise review on fundamental concepts of nanotechnology and applications in material science and technology. *Results in Chemistry*, *4*, 100633. https://doi.org/10.1016/j.rechem.2022.100633

Al-Hakkani, M. F., Gouda, G. A., & Hassan, S. H. A. (2021). A review of green methods for phyto-fabrication of hematite (α-Fe_2O_3) nanoparticles and their characterization, properties, and applications. *Heliyon*, *7*(1), e05806. https://doi.org/10.1016/j.heliyon.2020.e05806

Basumatary, S. F., Das, B., Das, B. K., Hoque, M., Brahma, S., Basumatary, B., … Basumatary, S. (2024). Recent advances in magnetic solid catalysts: Synthesis, stabilization and application in cleaner production of biodiesel. *Energy Nexus*, *15*, 100318. https://doi.org/10.1016/j.nexus.2024.100318

Chauhan, A., Rana, G., Dutta, V., Kumari, A., Krishna Rao, S., Subbarayan, R., … Ghotekar, S. (2024). Recent trends in phyto-mediated iron-based nanomaterials for environmental remediation and biomedical applications. *Inorganic Chemistry Communications*, *160*, 111976. https://doi.org/10.1016/j.inoche.2023.111976

Chellappa, M., & Vijayalakshmi, U. (2019). Fabrication of Fe_3O_4-silica core-shell magnetic nano-particles and its characterization for biomedical applications. *Materials Today: Proceedings*, *9*, 371–379. https://doi.org/ 10.1016/j.matpr.2019.02.166

Hong, R., Li, J., Wang, J., & Li, H. (2007). Comparison of schemes for preparing magnetic Fe_3O_4 nanoparticles. *China Particuology*, *5*(1), 186-191. https://doi.org/10.1016/j.cpart.2007.01.011

Iida, H., Takayanagi, K., Nakanishi, T., & Osaka, T. (2007). Synthesis of Fe_3O_4 nanoparticles with various sizes and magnetic properties by controlled hydrolysis. *Journal of Colloid and Interface Science*, *314*(1), 274–280. https://doi.org/10.1016/j.jcis.2007.05.047

Ji, D., Yang, H., Zhang, Q., Ding, H., Zhang, S., Zhang, G., & Pang, H. (2024). Iron series metal-organic frameworks and their composite nanomaterials: Controllable synthesis and clean energy applications. *Nano Energy*, *125*, 109559. https://doi.org/10.1016/j.nanoen.2024.109559

Jiao, D., Lesage, K., Yardimci, M. Y., El Cheikh, K., Shi, C., & De Schutter, G. (2021). Structural evolution of cement paste with nano-Fe_3O_4 under magnetic field-Effect of concentration and particle size of nano-Fe_3O_4. *Cement and Concrete Composites*, *120*, 104036. https://doi.org/10.1016/j.cemconcomp.2021.104036

Koizumi, H., Uddin, Md. A., & Kato, Y. (2021). Effect of ultrasonic irradiation on γ-Fe_2O_3 formation by co-precipitation method with Fe^{3+} salt and alkaline solution. *Inorganic Chemistry Communications*, *124*, 108400. https://doi.org/10.1016/j.inoche.2020.108400

Li, S., Huang, M., Cui, M., Jin, G., & Xu, K. (2024). Improving the thermal-mechanical performance of bio-treated backfill materials by addition of magnetic iron oxide nanoparticles (nano-Fe_3O_4). *Geomechanics for Energy and the Environment*, *39*, 100571. https://doi.org/10.1016/j.gete.2024.100571

Munoz, M., de Pedro, Z. M., Casas, J. A., & Rodriguez, J. J. (2015). Preparation of magnetite-based catalysts and their application in heterogeneous Fenton oxidation-A review. *Applied Catalysis B: Environmental*, *176–177*, 249-265. https://doi.org/10.1016/j.apcatb.2015.04.003

Niu, Y., Zhang, X., Kang, Y., Sun, P., Liu, H., Xiao, Z., & Zhao, D. (2024). Magnetic microcapsules based on Fe_3O_4 nanoparticles: Preparation, properties, and applications. *Materials Today Communications*, *39*, 108660. https://doi.org/10.1016/j.mtcomm.2024.108660

Pavithra, N., Nirmala, M., Priyadharshini, S., Kavitha, U., & Kavitha, B. (2024). Influence of pH on structural, optical and magnetic properties of undoped and Ni-doped α-Fe_2O_3 nanoparticles for antimicrobial activity. *Nano-Structures & Nano-Objects*, *37*, 101098. https://doi.org/10.1016/j.nanoso.2024.101098

Prasetya, D. (2018). *Efek pengadukan dan variasi ph pada sintesis Fe_30_4 dari pasir besi dengan metode kopresipitasi*. Institut Teknologi Sepuluh Nopember, Surabaya.

Revathy, R., Sajini, T., Augustine, C., & Joseph, N. (2023). Iron-based magnetic nanomaterials: Sustainable approaches of synthesis and applications. *Results in Engineering*, *18*, 101114. https://doi.org/10.1016/j.rineng.2023.101114

Wang, H., Jiang, X., Qin, Y., Xiong, Z., & Zhao, L. (2024). Research trends in functionalized Fe3O4 composites based on affinity recognition systems for targeted extraction of natural products. *Journal of Chromatography A*, *1730*, 465145. https://doi.org/10.1016/j.chroma.2024.465145

Wang, L., Huang, X., Wang, C., Tian, X., Chang, X., Ren, Y., & Yu, S. (2021). Applications of surface functionalized Fe_3O_4 NPs-based detection methods in food safety. *Food Chemistry*, *342*, 128343. https://doi.org/10.1016/j.foodchem.2020.128343

Xu, J., Yang, H., Fu, W., Du, K., Sui, Y., Chen, J., … Zou, G. (2007). Preparation and magnetic properties of magnetite nanoparticles by sol–gel method. *Journal of Magnetism and Magnetic Materials*, *309*(2), 307–311. https://doi.org/10.1016/j.jmmm.2006.07.037

Zhou, Y., Yang, X., Gong, C., Zhu, F., Wang, J., Qi, Y., … Liu, Y. (2023). Recent progress in γ-Fe_2O_3-based catalysts: An overview of the synthesis and applications in environmental remediation. *Chemical Engineering Journal*, *475*, 146198. https://doi.org/10.1016/j.cej.2023.146198